Inorganic Chemistry

Article

pubs.acs.org/IC

Iron Coordination Chemistry with New Ligands Containing Triazole and Pyridine Moieties. Comparison of the Coordination Ability of the N-Donors

Nathalie Ségaud,[†] Jean-Noël Rebilly,*[,‡] Katell Sénéchal-David,[†] Régis Guillot,[†] Laurianne Billon,[†] Jean-Pierre Baltaze,[†] Jonathan Farjon,[†] Olivia Reinaud,[‡] and Frédéric Banse*[,†]

[†]Institut de Chimie Moléculaire et des Matériaux d'Orsay, Université Paris Sud, F-91405 Orsay, France

[‡]Laboratoire de Chimie et de Biochimie Pharmacologiques et Toxicologiques, Université Paris Descartes, CNRS UMR 8601, F-75270 Paris Cedex 06, France

Supporting Information

ABSTRACT: We report the synthesis, characterization, and solution chemistry of a series of new Fe^{II} complexes based on the tetradentate ligand *N*-methyl-*N*,*N*′-bis(2-pyridyl-methyl)-1,2-diaminoethane or the pentadentate ones *N*,*N*′,*N*′-tris(2-pyridyl-methyl)-1,2-diaminoethane and *N*,*N*′,*N*′-tris(2-pyridyl-methyl)-1,3-diaminopropane, modified by propynyl or methoxyphenyltriazolyl groups on the amino functions. Six of these complexes are characterized by X-ray crystallography. In particular, two of them exhibit an hexadentate coordination environment around Fe^{II} with two amino, three pyridyl, and one triazolyl groups. UV−visible and cyclic voltammetry experiments of acetonitrile solutions of the complexes allow to deduce accurately the structure of all Fe^{II} species in equilibrium. The stability of the complexes could be ranked as follows: $[L_5Fe^{II}\text{-py}]^{2+}$ > $[L_5Fe^{II}\text{−Cl}]^{+}$ > $[L_5Fe^{II}\text{-triazolyl}]^{2+}$ > $[L_5Fe^{II}\text{-(NCMe)}]^{2+}$, where L_5 designates a pentadentate coordination sphere composed of the two amines of ethanediamine and three pyridines. For complexes based on propanediamine, the hierarchy determined is $[L_5Fe^{II}\text{−Cl}]^{+}$ > $[L_5Fe^{II}\text{(OTf)}]^{+}$ > $[L_5Fe^{II}\text{-(NCMe)}]^{2+}$, and no ligand exchange could be evidenced for $[L_5Fe^{II}\text{-triazolyl}]^{2+}$. Reactivity of the $[L_5Fe^{II}\text{-triazolyl}]^{2+}$ complexes with hydrogen peroxide and PhIO is similar to the one of the parent complexes that lack this peculiar group, that is, generation of $Fe^{III}(OOH)$ and $Fe^{IV}(O)$, respectively. Accordingly, the ability of these complexes at catalyzing the oxidation of small organic molecules by these oxidants follows the tendencies of their previously reported counterparts. Noteworthy is the remarkable cyclooctene epoxidation activity by these complexes in the presence of PhIO.

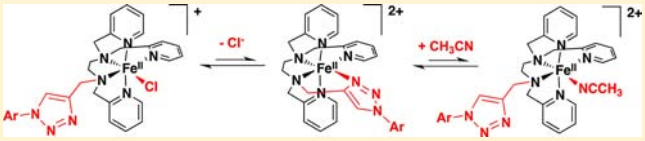

INTRODUCTION

Studies dedicated to non heme metalloenzyme modeling by synthetic iron complexes bearing simple neutral ligands containing N-donors are numerous. In particular, convincing results have been obtained implementing these complexes as precursors for reaction intermediates identified in the catalytic cycle of enzymes responsible for oxygen transfer reactions involved in biosynthesis or biodegradation processes.[1] In contrast, reports concerning the use of such complexes as metalloenzymes functional models, that is, complexes able to achieve large turnover numbers in aqueous medium are very rare if not nonexistent. Some obvious reasons are the fragility of some parts of the ligands under oxidative conditions[2] and, generally, the moderate solubility of the complexes in water. Collins et al. have developed a strategy to identify and to reinforce the weak sites of their ligands, which led them to devise efficient oxidation catalysts based on TAML ligands.[3] Another approach is to support the catalysts on solids. In our case, grafting of Fe^{II} complexes on silica surfaces allowed to observe catalytic oxidative degradation of 2,3,6-trichlorophenol by H_2O_2 with large turnover numbers. In addition, this strategy allowed the catalysts to be recovered.[4]

Considering the reputed advantages of the so-called "click chemistry",[5] works reporting surface immobilization of complexes via azide−alkyne cycloaddition are emerging, mainly for the study of reactions involving electron transfers.[6] The triazole resulting from the "click" synthesis being a potential ligand for the metal center, in particular Fe^{II},[7] a preliminary task for the surface tethering is to determine whether or not the triazole modifies the complex characteristics, in particular when a catalytic function of the device is sought.

Herein, we report the solid state characterization and solution coordination chemistry of Fe^{II} with some of our standard amine/pyridine ligands modified with a triazole moiety that could compete with pyridines for the binding to the metal center. Reaction of some of these Fe^{II} precursors with chemical oxidants to generate oxidizing reaction intermediates or to run catalytic assays allows to further illustrate the similarities and differences between these new complexes and the parent ones.

Received: August 22, 2012
Published: January 9, 2013

   dx.doi.org/10.1021/ic301834x | *Inorg. Chem.* 2013, 52, 691−700

RESULTS AND DISCUSSION

Synthesis of the Ligands. All ligands are built on a diamine fragment (ethane- or propanediamine) on which pyridyl, triazolyl, or non coordinating groups such as methyl or propynyl were grafted. Upon reaction between propargyl bromide and tetradentate or pentadentate ligands containing one secondary amine, the ligands mpL_4^2, pL_5^2, and pL_5^3 (see Chart 1) were obtained as described in the Experimental Section. Implementation of the Cu^I-catalyzed azide–alkyne procedure between the former molecules and 1-azido-4-methoxybenzene led to mtL_4^2, tL_5^2, and tL_5^3 (see Chart 1). In our nomenclature, the superscript 2 or 3 indicates that the ligand is based on ethanediamine or propanediamine, respectively. The subscript 4 or 5 indicates the total number of amine and pyridine functions, and the prefix m, p, or t stands for a methyl, a propynyl, or a triazolyl group, respectively. Note that, according to these rules, the long studied TPEN ligand[8] should be named L_6^2.

Chart 1. Structure and Numbering of the Ligands[8] Used in This Study

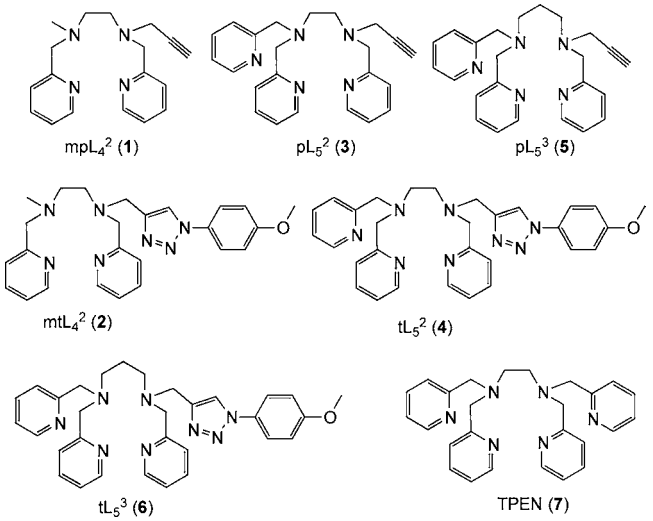

Synthesis and Solid State Characterization of Fe^{II} Complexes. The six ligands then obtained were used to prepare nine Fe^{II} complexes in the presence of strongly or poorly coordinating anions ($FeCl_2$ or $Fe(OTf)_2$, respectively, see Experimental Section) denoted as complexes of **a** or **b** type in the following. Six of those complexes were structurally characterized by X-ray crystallography (cf. Figure 1). A similar structural motif is observed in each structure, that is, two equatorial amine and two axial pyridine donors around Fe^{II}. For all of the complexes, the coordination sphere is completed either by equatorial anions (chloride or triflate) or nitrogen donors (pyridine or triazole) or both. For the complexes that contain at least one anionic ligand, the Fe–N bond lengths are about 2.2 Å (cf. Supporting Information), which is indicative of a high spin Fe^{II}. In contrast, complexes $[(tL_5^2)Fe](PF_6)_2$ (**4b**) and $[(tL_5^3)Fe](PF_6)_2$ (**6b**) hold a low spin Fe^{II} as revealed by shorter Fe–N bonds of about 2 Å.[9] Note that ferrous ions surrounded by 6 neutral N frequently undergo spin state equilibrium.[2b,10] Therefore, the latter conclusion is true under the experimental conditions of X-ray diffraction, that is, at 100 K.

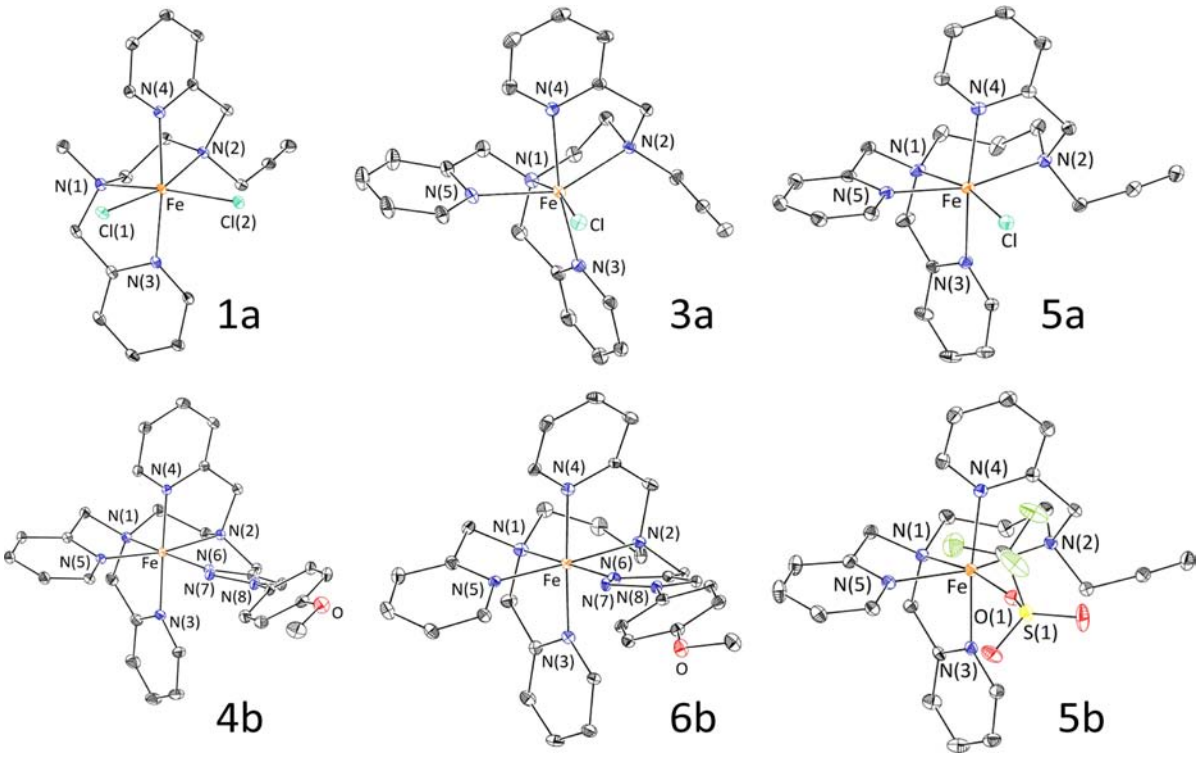

Figure 1. ORTEP diagram (30% probability thermal ellipsoids) of Fe^{II} complexes showing the atom-numbering scheme. **1a** $(mpL_4^2)FeCl_2$, **3a** $[(pL_5^2)FeCl](PF_6)$, **5a** $[(pL_5^3)FeCl](PF_6)$, **4b** $[(tL_5^2)Fe](PF_6)_2$, **6b** $[(tL_5^3)Fe](PF_6)_2$, and **5b** $[(pL_5^3)Fe(OTf)](OTf)$. Hydrogen atoms, solvent molecules, and counteranions have been omitted for clarity.

dx.doi.org/10.1021/ic301834x | Inorg. Chem. 2013, 52, 691–700

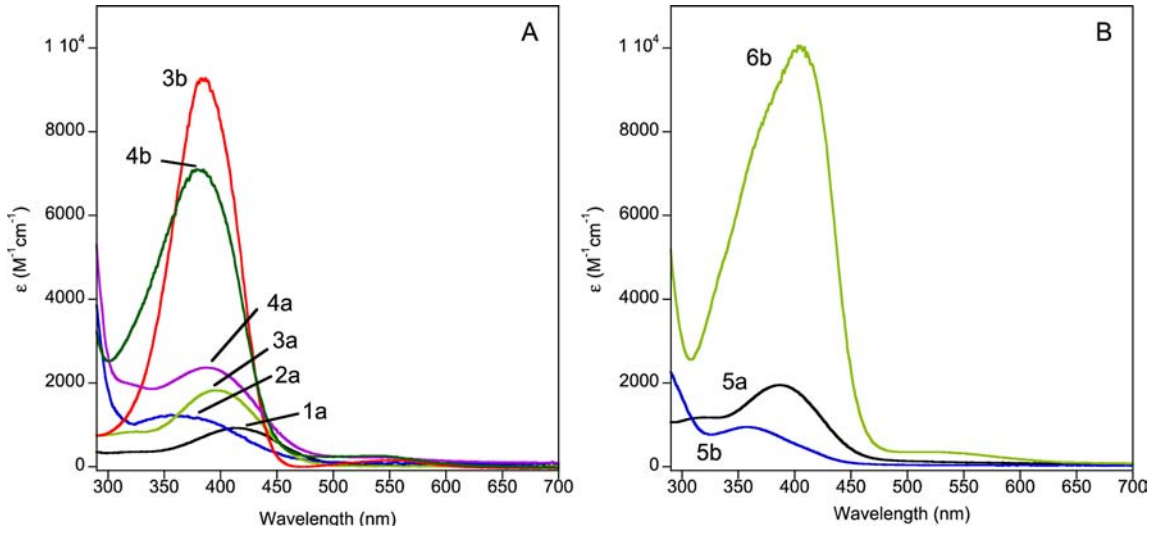

Figure 2. Visible absorption spectra in acetonitrile of (A) complexes **1a** (black), **2a** (blue), **3a** (light green), **3b** (red), **4a** (purple), and **4b** (dark green) ; and of (B) **5a** (black), **5b** (blue), and **6b** (light green).

Table 1. Spectrophotometric and Electrochemical Data Observed for the Solids Dissolved in Acetonitrile, and Nature of the Complexes Then Determined[a]

sample	λ_{max}[b] (extinction coefficient)	$E_{1/2}$ (mV), ΔE[b]	nature of complexes[c,d]
$(mpL_4^2)FeCl_2$ **1a**	416 (900)	248 (90)	N_4FeCl_2[c,d]
$(mtL_4^2)FeCl_2$ **2a**	370 (1200)	225 (85); 568 (75)	N_4FeCl_2[c,d]
			N_5FeCl^{+}[c,d]
$[(pL_5^2)FeCl](PF_6)$ **3a**	396 (1800)	651 (85); 1010 (85)	N_5FeCl^{+}[c,d]
			$N_5Fe(MeCN)^{2+}$[d]
$[(tL_5^2)FeCl](PF_6)$ **4a**	390 (2400)	610 (70); 827 (75)	N_5FeCl^{+}[c,d]
			N_6Fe^{2+}[c,d]
$[(pL_5^3)FeCl](PF_6)$ **5a**	389 (1900)	721 (90)	N_5FeCl^{+}[c,d]
$[(pL_5^2)Fe(OTf)](OTf)$ **3b**	385 (9200)	1016 (90)	$N_5Fe(MeCN)^{2+}$[c,d]
$[(tL_5^2)Fe](PF_6)_2$ **4b**	381 (7000)	827 (90); 1035 (70)	N_6Fe^{2+}[c,d]
			$N_5Fe(MeCN)^{2+}$[c,d]
$[(pL_5^3)Fe(OTf)](OTf)$ **5b**	360 (950)	733 (75); 1130 (100)	$N_5Fe(OTf)l^{+}$[c,d]
			$N_5Fe(MeCN)^{2+}$[d]
$[(tL_5^3)Fe](PF_6)_2$ **6b**	406 (10 000)	870 (85)	N_6Fe^{2+}[c,d]

[a] N_x stands for a coordination sphere comprising an ancillary ligand with x neutral ligands such as amino, pyridyl, and triazolyl. [b] Absorption wavelength are given in nm, extinction coefficient in M^{-1} cm^{-1}, potential values in mV vs saturated calomel electrode (SCE). [c] Complex observed by UV−visible. [d] Complex observed by cyclic voltametry.

Characterization of the Fe^{II} Complexes in Solution. When dissolved in acetonitrile, the complexes are light yellow to dark red colored. Determining their structure in solution by means of NMR is not straightforward. Indeed, the paramagnetic character of Fe^{II} induces signal broadenings that prevent sufficient sensitivity and spectral resolution for analyzing nuclei of interest, such as ^1H (cf. Supporting Information). However, systematic comparisons between electronic absorption spectra and cyclic voltammograms of related complexes allows to readily evidence the metal coordination sphere.

For each complex, the electronic absorption spectrum exhibits a very strong absorption in the UV, corresponding mainly to pyridines $\pi-\pi^*$ transitions, and a less intense one in the visible related to Fe^{II} t_{2g}-to-pyridine π^* charge transfers that are responsible for the color of the solution (cf. Figure 2). For closely related Fe^{II} complexes, it is possible to infer the first coordination sphere in solution from the position and intensity of the MLCT.[9b] However, the conclusions have to be taken with care since chemical equilibria between several complexes may occur in solution. In that case, the absorptions observed are obviously a convolution of the contribution of the separate complexes.

The parent complex of $(mpL_4^2)FeCl_2$ (**1a**), $(m_2L_4^2)FeCl_2$, has been shown to preserve its structure in solution.[11] Since the metal-to-ligand charge-transfer (MLCT) of **1a** (416 nm, 900 M^{-1} cm^{-1}) is very similar to the one of $(m_2L_4^2)FeCl_2$, it can be deduced that **1a** exhibits the same structure both in the solid state and in acetonitrile. By comparison, the absorption band of $[(pL_5^2)FeCl](PF_6)$ (**3a**) (396 nm, 1800 M^{-1} cm^{-1}) is more intense and lies higher in energy, which is compatible with the coordination of a strong π accepting pyridine in place of a chloride. For $[(pL_5^2)Fe(OTf)](OTf)$ (**3b**), the band (385 nm, 9200 M^{-1} cm^{-1}) is even more intense and displaced to higher energy. With respect to **3a**, this can be assigned to the replacement of the chloride by a stronger field σ-donor and π-accepting ligand such as acetonitrile, leading to a low spin Fe^{II} center. This conclusion is fully compatible with the one drawn from the study of $[(mL_5^2)FeCl](BPh_4)$ and $[(mL_5^2)Fe(OH_2)](BPh_4)_2$,[9b] where mL_5^2 is identical to the ligand pL_5^2 but with a

dx.doi.org/10.1021/ic301834x | Inorg. Chem. 2013, 52, 691−700

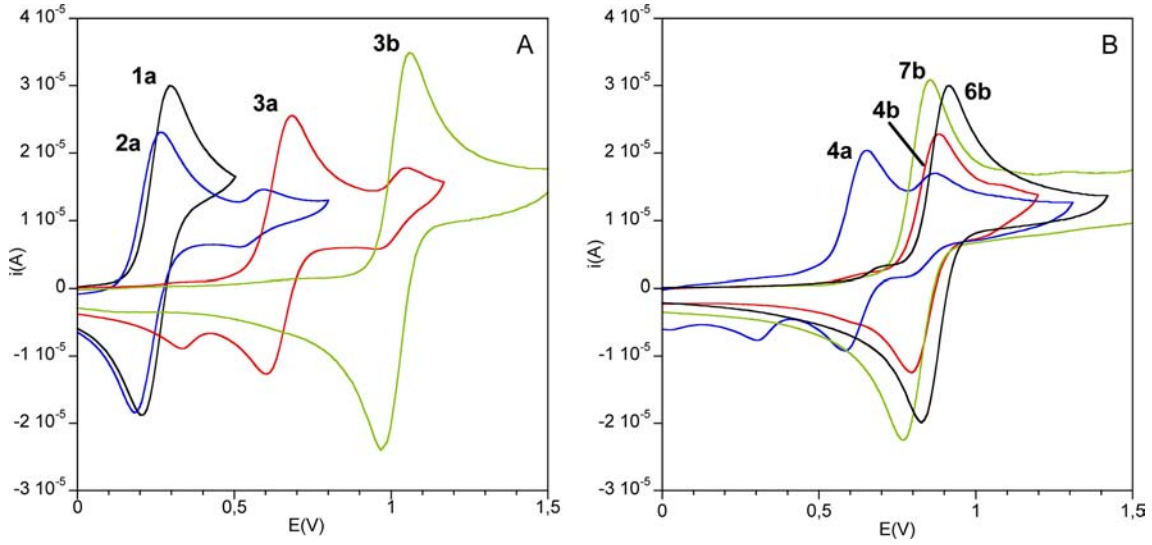

Figure 3. Cyclic voltamograms of about 2 mM solutions of the Fe^{II} complexes in acetonitrile at room temperature at a scan rate of 100 mV s^{-1}. (A) $(mpL_4^2)FeCl_2$ **1a** (black), $(mtL_4^2)FeCl_2$ **2a** (blue), $[(pL_5^2)FeCl](PF_6)$ **3a** (red), $[(pL_5^2)Fe(OTf)](OTf)$ **3b** (green); and of (B) $[(tL_5^2)FeCl](PF_6)$ **4a** (blue), $[(tL_5^2)Fe](PF_6)_2$ **4b** (red), $[(tL_5^3)Fe](PF_6)_2$ **6b** (black), $[(TPEN)Fe^{II}](PF_6)_2$ **7a** (green). A glassy carbon electrode as a working electrode and saturated calomel electrode as a reference were used. Tetrabutylammonium hexafluorophosphate (0.1M) was used as supporting electrolyte.

methyl group instead of the propynyl one. For $[(tL_5^2)Fe](PF_6)_2$ (**4b**), the MLCT band is observed at 381 nm and with a large intensity (7000 M^{-1} cm^{-1}) which is compatible with the structure determined by X-ray diffraction (cf. Figure 1) or with an acetonitrile in place of the triazole as in **3b**. $[(tL_5^2)FeCl](PF_6)_2$ (**4a**) displays spectroscopic features (390 nm, 2400 M^{-1} cm^{-1}) intermediate between **3a** and **4b**. Therefore, one can propose that complex **4a** undergoes a chemical equilibrium in acetonitrile. In one fraction of the complex the Fe^{II}–Cl bond is preserved whereas the chloro ligand is substituted by a stronger field one, such as acetonitrile or the triazole moiety, in the other fraction. For complex $(mtL_4^2)FeCl_2$ (**2a**), the MLCT band is very broad and observed at a lower wavelength but a larger intensity (370 nm, 1200 M^{-1} cm^{-1}) than that of $(mpL_4^2)FeCl_2$ **1a**. The broadness may be related to the presence of two complexes in equilibrium, one exhibiting a coordination sphere similar to **1a** with the triazole fragment dangling and the second one where the triazole would substitute one chloro ligand. Such a substitution should be accompanied by a blue shift and an increase of the extinction coefficient, as observed for **2a**.

The complexes with the ligands based on the propanediamine fragment (**5** and **6**) were also studied in acetonitrile. $[(tL_5^3)Fe](PF_6)_2$ (**6b**) displays a MLCT at 406 nm (10000 M^{-1} cm^{-1}) (cf. Figure 2). The same was observed in MeOH (not shown). Therefore, one can conclude that the structure observed in the solid state is conserved in solution, that is, with the 6 nitrogen atoms from the ligand coordinated to Fe, including the triazole group. In acetonitrile, $[(pL_5^3)FeCl](PF_6)$ (**5a**) displays a band at 389 nm with an extinction coefficient of 1900 M^{-1} cm^{-1} that corresponds to a high spin ($S = 2$) Fe^{II} center. This is similar to **3a** (cf. Table 1). Therefore, it is most likely that **5a** exhibits the same structure in solution and in the solid state, that is, with the pentadentate N ligand wrapping the metal center and a chloro to complete the pseudo octahedral coordination sphere. For $[(pL_5^3)Fe(OTf)](OTf)$ (**5b**), the absorption is observed at 360 nm with a weaker intensity (950 M^{-1} cm^{-1}). One would expect that the triflate ligand observed in the crystal structure of **5b** is substituted by acetonitrile yielding a low spin Fe^{II} complex. However, the low extinction coefficient is rather compatible with a high spin Fe^{II}. As a consequence, it is plausible that the Fe^{II}-triflate bond remains in solution. With respect to **5a**, the blue shift of the MLCT band may be due to the presence of a weak π donating triflate instead of a chloride.

All these data are summarized in Table 1. They indicate that for complexes with ligands containing a triazole moiety (**2a**, **4a**, **4b**, and **6b**) its coordination to the metal center is effective. Even though it is considered as a poor ligand with respect to Cl^-, examination of the position and intensity of the MLCT suggests that a competition between both ligands operates for **2a** and **4a**. Note that a chelate effect will benefit to the formation of the triazole-Fe bond.

Probing every redox active species, cyclic voltametry provides a more accurate description of the different complexes present in acetonitrile solution. Since we aim at using these Fe^{II} complexes as oxidation catalysts, our purpose is here to identify all of these species as they are potential precursors for reaction intermediates. Minor cathodic processes that are sometimes formed following rearrangement of electrogenerated species will not be discussed in detail in the following.

Complexes $(mpL_4^2)FeCl_2$ **1a** and $(mtL_4^2)FeCl_2$ **2a** exhibit a very similar redox signature in the positive range with respect to saturated calomel electrode (SCE) (cf. Figure 3A). This reversible signal is observed at $E_{1/2}$ 248 mV and 225 mV for **1a** and **2a**, respectively. Another quasi reversible wave is observed at a potential of 568 mV for **2a** confirming that two complexes are in equilibrium. It is reasonable to assign the signal at low potential to the Fe^{III}/Fe^{II} redox potential for structures identical to the one of **1a** observed in the solid state (cf. Figure 1), that is, with the metal center coordinated by the four N atoms from the ancillary ligand and two chlorides. This assignment is compatible with potential values measured for complexes similar to **1a**.[11,12] The other wave observed for **2a** can be due to a structure in which the triazole substitues a chloro ligand. Giving rise to a change of the complex charge from zero to +1, this ligand exchange would lead to an increase

dx.doi.org/10.1021/ic301834x | *Inorg. Chem.* 2013, 52, 691−700

Scheme 1. Fe^{III}/Fe^{II} Potential Value Ranges as a Function of the Coordination Sphere of Complexes $(mtL_4^2)FeCl_2$ 2a, $[(pL_5^2)FeCl](PF_6)$ 3a, $[(pL_5^2)Fe(OTf)](OTf)$ 3b, $[(tL_5^2)FeCl](PF_6)$ 4a, $[(tL_5^2)Fe](PF_6)_2$ 4b, $[(pL_5^3)FeCl](PF_6)$ 5a, $[(pL_5^3)Fe(OTf)](OTf)$ 5b, $[(tL_5^3)Fe](PF_6)_2$ 6b, and $[(TPEN)Fe](PF_6)_2$ 7a[a]

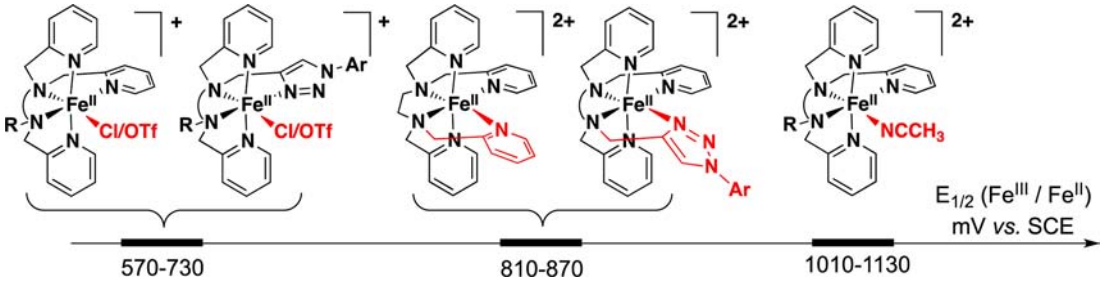

[a]Values are determined in acetonitrile with respect to saturated calomel electrode. R stands for any group not coordinated to Fe, Ar designates the methoxyphenyl substituent of the triazole moiety.

of the potential value as well, which is consistent with the observation. Thus, extending our nomenclature (see above) the ligand mtL_4^2 is able to behave as a mL_5^2 one (cf. Scheme 2), which is consistent with the UV−visible data.

For $[(pL_5^2)FeCl](PF_6)$ **3a**, the major signal at $E_{1/2}$ 651 mV can be attributed to the redox process between **3a** and its one-electron oxidized form (i.e., $[(pL_5^2)Fe^{III/II}Cl]^{2+/+}$), which is in agreement with complexes where Fe is in a similar coordination sphere.[9a] The wave observed at higher potential (1.02 V) lies at a value identical to the only one of $[(pL_5^2)Fe(OTf)](OTf)$ **3b** (see Table 1). For this latter, the pentadentate 2 amines/3 pyridines Fe^{II} coordination sphere is completed by an acetonitrile molecule, as indicated by UV−visible absorption spectroscopy (see above). Therefore, the quasi reversible wave at high potential for **3a** is related to the $[(pL_5^2)Fe^{III/II}(NCMe)]^{3+/2+}$ redox couple. This attribution is also in agreement with the electrochemical data reported for $[(N4Py)Fe^{II}(MeCN)]^{2+}$.[13] Note that the existence of this latter form, most likely giving rise to a low spin Fe^{II}, was not inferred from the spectrophotometric characterization of **3a**. However, the relative intensities of the two anodic peaks show that the amount of the $[(pL_5^2)Fe^{II}Cl]^+$ complex is much higher. Thus, it is likely that the spectroscopic feature of $[(pL_5^2)Fe^{II}(MeCN)]^{2+}$ is hidden by that of $[(pL_5^2)FeCl]^+$ (see Scheme 2). On the reverse scan, a peak at 0.33 V is observed. Bernal et al. reported a similar signal for $[(mL_5^2)Fe^{II}Cl]^+$ and suggested that this additional wave indicates a rapid rearrangement of Fe^{III} species generated at the electrode.[14] For $[(mL_5^3)Fe^{II}Cl]^+$, such a signal was assigned to the reduction of $[(mL_5^3)Fe^{III}(OH)]^{2+}$ formed in the presence of residual water.[15] A similar attribution can be proposed here for **3a**, but also for **4a** (see below).

In the case of $[(tL_5^2)FeCl](PF_6)$ **4a** two signatures corresponding to two Fe^{III}/Fe^{II} couples are observed (cf. Figure 3B). The major redox couple is characterized by $E_{1/2}$ 610 mV. By comparison with **3a**, this can be assigned to the process $[(tL_5^2)Fe^{II}Cl]^+ \leftrightarrow [(tL_5^2)Fe^{III}Cl]^{2+}$. The minor signal observed at 827 mV is close from the $E_{1/2}$ values of 827 and 870 mV measured for $[(tL_5^2)Fe](PF_6)_2$ **4b** and $[(tL_5^3)Fe](PF_6)_2$ **6b**, respectively. The rationale is obviously related to the similarity of the metal coordination sphere in these species. Thus, for these three complexes the signal at about 830−870 mV is attributed to $[(L_6)Fe^{III/II}]^{3+/2+}$ redox couples arising from the coordination of the triazole moiety to Fe. Accordingly, these values lie also in the range reported for Fe^{III}/Fe^{II} complexes bearing hexadentate 2 amine/4 pyridine ligands such as TPEN (814 mV) but are slightly higher (see Table 1). Therefore, pyridine has a better donating ability than triazole. Note that the very weak signal at $E_{1/2}$ 1035 mV detected for **4b** can be assigned to a complex where acetonitrile substitutes the triazolyl group, which indicates that, in turn, the latter is a better donor than the solvent.

For $[(pL_5^3)FeCl](PF_6)$ **5a**, only one redox signal is observed at $E_{1/2}$ 721 mV (cf. Supporting Information), which is 70 mV higher than that of **3a**. This about 70 mV difference between Fe^{III}/Fe^{II} complexes surrounded by ligands only differing by the diamine bridge (i.e., ethanediamine vs propanediamine) has already been noted.[15] Thus, this strongly suggests that the structure of **5a** determined by X-ray diffraction is not modified upon dissolution. For $[(pL_5^3)Fe(OTf)](OTf)$ **5b**, a first wave is observed at $E_{1/2}$ 733 mV and a second one of higher intensity at $E_{1/2}$ 1130 mV. These values are similar to those of **3a** and **3b**, respectively. Then, the higher potential one can be attributed to the $[(pL_5^3)Fe^{III/II}(MeCN)]^{3+/2+}$ redox couple. Regarding the other wave, it can be assigned to a redox couple involving a monocationic ferrous complex as observed for **2a**, **3a**, **4a**, and **5a**. By contrast with these species, the only anion available in **5b** is a triflate and not a chloro. Therefore, an equilibrium between $[(pL_5^3)Fe^{II}(MeCN)]^{2+}$ and $[(pL_5^3)Fe^{II}(OTf)]^+$ is here evidenced. Even though triflate is considered very labile, it can bind to the metal center as seen in the crystal structure of **5b** (cf. Figure 1). A discrepancy with UV−visible spectroscopy appears here in that the presence of $[(pL_5^3)Fe^{II}(MeCN)]^{2+}$ was not deduced. Monitoring separately the two complexes by electronic spectroscopy may help in explaining this dissimilarity.

Finally, all these results can be summarized in Scheme 1. Except for **1a**, all the complexes exhibit structures in acetonitrile solution where the Fe^{II} is surrounded by at least 5 nitrogen ligands, the sixth ligand being either an anion (chloride or triflate), or a neutral nitrogen donor (pyridine, triazole or acetonitrile). For most of them the 5 N ligands are two amino and three pyridine ligands, or two amino, two pyridines, and a triazole in **2a**. This leads to distinct $E_{1/2}$ ranges for the Fe^{III}/Fe^{II} couples depending on both the charge of the ferrous complex as well as the donating ability of the sixth ligand. With an anion to complete the coordination sphere, the redox potentials are observed between 570 and 730 mV for **2a**, **3a**, **4a**, **5a**, and **5b** (cf. Table 1). With a pyridine or a triazole donor, the potential values lie between 810 and 870 mV for **4a**, **4b**, **6b**, and **7a**. For **3a**, **3b**, and **5b**, where the poor donor acetonitrile completes the coordination sphere the redox potentials are observed at values larger than 1 V vs SCE.

dx.doi.org/10.1021/ic301834x | Inorg. Chem. 2013, 52, 691−700

Comparison of the data collected for the whole complexes in acetonitrile solution allows to propose a ranking for the affinity of the studied ligands for Fe^{II} in our complexes. As depicted in Scheme 2, evidence have been obtained that for complexes with

Scheme 2. Representation of the Ligand Exchanges Evidenced in Acetonitrile Solution for the Complexes Bearing Pentadentate (N_5) or Hexadentate (N_6) Ligands Based on the Ethanediamine Backbone[a]

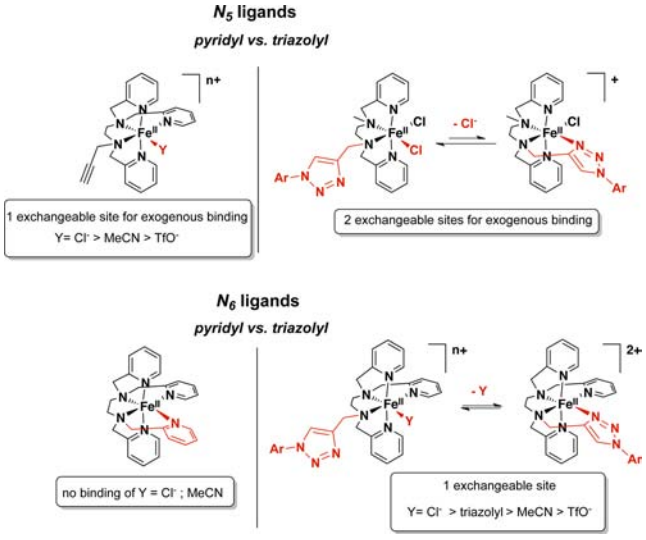

[a]Comparison between complexes containing pyridyl and triazolyl arms.

ligands based on ethanediamine equilibria occur between Fe^{II}–Cl and Fe^{II}-triazolyl species (complexes **2a** and **4a**). However, the Fe^{II}–Cl bond is always favored over the Fe^{II}-triazolyl one. In addition, the solvent acetonitrile is able to participate in the coordination to Fe^{II}, but it is a much poorer ligand than the others, as seen for **3a** and **4b**. Finally, the pyridyl group is the best donor as all indicates that it stays bound to Fe^{II} in any case. Thus, the proposed classification in acetonitrile solvent is Fe^{II}-py > Fe^{II}–Cl > Fe^{II}-triazolyl > Fe^{II}–NCMe. It has been shown that 1,4-disubstituted-1,2,3-triazole are versatile ligands, depending on the nature of their substituents.[7b,16] Therefore, the above order is only valid under the present conditions. For Fe^{II} complexes with propanediamine based ligands, no exchange could be observed in the presence of the triazolyl moiety in **6b**. In contrast, examination of **5a** and **5b** reveals the following affinity Fe^{II}–Cl > Fe^{II}–OTf > Fe^{II}–NCMe.

Reactivity of Some of the Fe^{II} Complexes with Chemical Oxidants. The reaction with chemical oxidants of parent complexes of those bearing the triazole group to generate reaction intermediates such as $Fe^{III}(OOH)$[9,14,15,17] and $Fe^{IV}(O)$[2,18] has been previously reported. In addition, the same complexes have been used as catalysts for the oxidation of hydrocarbon by hydrogen peroxide or single oxygen atom donor such as PhIO or *m*CPBA.[18a,19] To determine whether or not, the triazole moiety perturbs the reactivity, complex $[(tL_5^2)Fe](PF_6)_2$ **4b** has been assayed with hydrogen peroxide and PhIO and compared with $[(tL_5^2)FeCl](PF_6)$ **4a**.

In a typical reaction to generate a $Fe^{III}(OOH)$ intermediate, the Fe^{II} precursor (1 mM in MeOH at 0 °C) was reacted with 30 equiv of H_2O_2. Monitoring of the reaction by UV–visible allowed to observe the progressive formation of the species, as seen in Figure 4 for **4b**. The characteristic HOO^--to-Fe^{III}

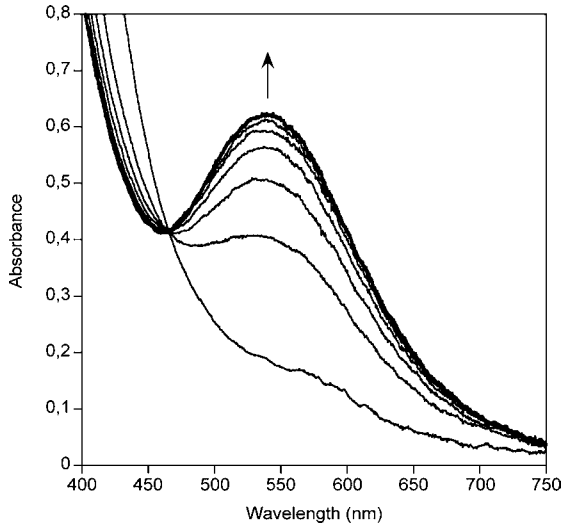

Figure 4. Formation of $[(tL_5^2)Fe^{III}(OOH)]^{2+}$ monitored by UV–visible at 0 °C, obtained by reaction of precursor **4b** (1 mM in MeOH) with 30 equiv of H_2O_2.

charge transfer was observed at 538 nm which is very similar to the values reported for $[(L_5^2)Fe^{III}(OOH)]^{2+}$ and $[(TPEN)Fe^{III}(OOH)]^{2+}$; that is, 537 and 541 nm, respectively.[17b] This assignment was confirmed by electron paramagnetic resonance (EPR) since the chromophore is associated with a typical spectrum of $Fe^{III}(OOH)$ (two sets of *g* values at 2.22, 2.15, 1.97 and 2.18, 2.12, 1.97 corresponding presumably to rotation isomers,[20] cf. Supporting Information). Determination of the extinction coefficient of the 538-nm band by double integration of the EPR signal gave a value of 1100 M^{-1} cm^{-1}, which is in agreement with literature data.[1a,17b,21] Therefore, the 538-nm chromophore can be formulated as $[(tL_5^2)Fe^{III}(OOH)]^{2+}$. Starting from **4a**, the same UV–visible and EPR spectroscopic features (cf. Supporting Information) were observed but with a lower intensity, which is likely due to the presence of the competing chloride ligand.[22] Then, it is reasonable to conclude that the same $Fe^{III}(OOH)$ intermediate is obtained from both precursors. The triazole moiety being not bound to Fe^{II} in **4a**, it is most likely dangling away from the metal coordination sphere in $Fe^{III}(OOH)$. Considering the maximum intensity of the MLCT at 538 nm, the conversion is 56% and 32% starting from precursors **4b** and **4a**, respectively. Importantly, it has to be noted that no hydroxylation of the ligand could be evidenced by ESI-MS examination of reaction mixtures after degradation of the $Fe^{III}(OOH)$.

Reaction of the Fe^{II} complexes with PhIO (1.2 equiv vs Fe) in acetonitrile yielded transient species characterized by new spectroscopic features. Starting from **4b** at 0 °C, the new chromophore was observed at 738 nm (cf. Figure 5), which lies in the 730–756 nm range reported for $Fe^{IV}(O)$ complexes supported by pentadentate 2 amines/3 pyridyl ligands.[2,18a,23] The same reaction was performed with precursor **4a** at lower temperature (−35 °C) to accumulate an intermediate characterized by an absorption at 729 nm. In addition, a peak at *m*/*z* 296.0995 was detected by HR ESI-MS for both samples, whose position and isotopic distribution are consistent with the formulation $\{[(tL_5^2)Fe^{IV}(O)]\}^{2+}$ (cf. Supporting Information). Importantly, the *m*/*z* 296.0995 peak vanished as the chromophore decayed. In addition, no other Fe^{IV} species could be identifed and no O-atom insertion in the ligand was detected in the mass spectra for both samples. Considering that

dx.doi.org/10.1021/ic301834x | Inorg. Chem. 2013, 52, 691–700

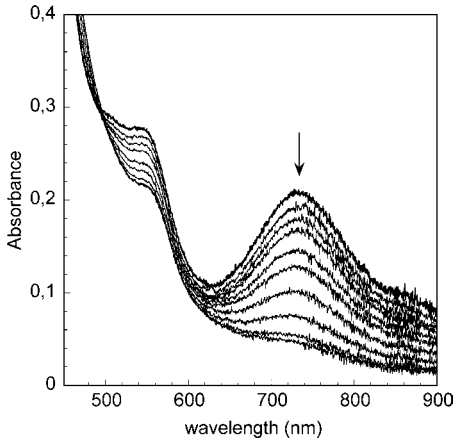

Figure 5. Degradation of $[(tL_5^2)Fe^{IV}(O)]^{2+}$ monitored by UV−visible at 0 °C over a 2 h 30 period. This intermediate was obtained from precursor **4b** (1 mM in MeCN) in the presence of 1.2 equiv of PhIO.

extinction coefficients are 300−400 M^{-1} cm^{-1} for such intermediates supported by neutral ligands,[2a,23,24] one can estimate a conversion in $Fe^{IV}(O)$ of 40% and 60% starting from **4a** and **4b**, respectively. Thus, this suggests that the same $Fe^{IV}(O)$ is generated from **4a** and **4b**. Therefore, the difference in the position of the absorption maxima observed for the *same* $Fe^{IV}(O)$ generated from each precursor could be due to the spectroscopic dissimilarities between them. Indeed, **4b** contains a low spin Fe^{II} with an intense MLCT at 381 nm and a side absorption at 550 nm (cf. Figures 2 and 5). By contrast, the MLCT is much less intense and no side absorption is observed in the case of the high spin Fe^{II} precursor **4a** (see Figure 2 and Supporting Information). The 550-nm side absorption persists after formation of $[(tL_5^2)Fe^{IV}(O)]^{2+}$ from **4b** which is consistent with an incomplete conversion into $Fe^{IV}(O)$. Then, overlapping between both bands may affect the $Fe^{IV}(O)$ feature.

Thus, these experiments show that the reactivity of the Fe^{II} complexes is not much altered by the triazole moiety. Such a conclusion is not so surprising since study of the Fe^{II} complexes in acetonitrile solution revealed that the Fe^{II}-triazole bond is not a tight one. However, it is noticeable that the conversion in $Fe^{III}(OOH)$ and $Fe^{IV}(O)$ complexes is lower than with the parent systems.[2b,9a,17b] Accordingly, here the reactions were performed at lower temperature to accumulate and identify the intermediates.

Small Molecule Oxidation Catalyzed by 4a, 4b, and 6b. To compare the catalytic efficiency of **4a**, **4b**, and **6b** with respect to their parent complexes that we studied in the past, three probe substrates were used: anisole, cyclooctene, and cyclohexane. The results obtained by gas chromatographic analyses of the reaction mixtures are given in Table 2.

Oxidation of anisole by hydrogen peroxide catalyzed by the Fe^{II} complexes led to products of aromatic hydroxylation with moderate to good yields and a large *ortho-*/*para-* regioselectivity, under either aerobic or anaerobic conditions. Similar results were observed when the parent complexes were used as catalysts.[19,25] In line with the reactivity of the Fe^{II} precursors with hydrogen peroxide (see above), this reaction was shown to be initiated by low spin $Fe^{III}(OOH)$ that afford the caged active species $[Fe^{IV}(O)$ + HO°$]$.[26] The lower yield of *ortho*-methoxyphenol obtained with **4a** may be related to the

Table 2. Oxidation of Anisole, Cyclooctene, and Cyclohexane by Hydrogen Peroxide and Iodosylbenzene Catalyzed by 4b and 6b in Acetonitrile at Room Temperature[a]

		$[(tL_5^2)FeCl](PF_6)$ **4a**		$[(tL_5^2)Fe](PF_6)_2$ **4b**		$[(tL_5^3)Fe](PF_6)_2$ **6b**	
		H_2O_2	PhIO	H_2O_2	PhIO	H_2O_2	PhIO
anisole[b]	*o*-OH	4		24		17	
	p-OH			1		1	
	PhOH	<1	1	<1	2	<1	1
cyclooctene[c]	epoxide	20	44	19	55	17	58
	diol	2		<1		1	
cyclohexane[d]	-ol	9	1	20	2	17	
	-one	9		17		23	

[a]Yields are given with respect to the oxidant. [b]Fe/H_2O_2/anisole: 1/20/3000, Fe/PhIO/anisole: 1/2/3000. The *ortho-* and *para*-methoxyphenols are denoted *o*-OH and *p*-OH, respectively. [c]Fe/H_2O_2/cyclooctene: 1/20/800, Fe/PhIO/cyclooctene: 1/2/800. Cyclooctene oxide and cyclooctane-1,2-diol are denoted epoxide and diol, respectively. [d]Fe/H_2O_2/cyclohexane: 1/20/800, Fe/PhIO/cyclooctene: 1/2/800. Cyclohexanol and cyclohexanone are denoted -ol and -one, respectively. All assays were performed under aerobic conditions.

presence of the chloro ligand leading to a lower conversion in $Fe^{III}(OOH)$ (see the previous section).

For cyclooctene, hydrogen peroxide led to one major product, cyclooctene oxide, and traces of *cis*-diol products. *Cis*-diol products are frequently obtained with Fe^{II} catalysts supported by tetradentate amine/pyridine ligands.[27] In that case, the oxidizing agent is a $Fe^{V}(O)(OH)$ intermediate[1c] that is proposed to be formed upon heterolytic cleavage of the former $Fe^{III}(OOH)$ providing two labile *cis* sites in the coordination sphere of Fe are available for peroxide activation. Such a situation is highly unlikely with the complexes here studied. With pentadentate bispidine-based Fe complexes, it was reported that epoxide and diol products were probably formed after homolytic cleavage of the FeO−OH to afford $Fe^{IV}(O)$ + HO°, the ferryl affording directly the epoxide or the diol when it is assisted by then hydroxyl radical.[28] The same scheme, that is not in contradiction with the aromatic hydroxylation pathway, may apply here, but more detailed studies are necessary to decipher the real mechanism. Note that the similarity between the results observed with the 3 catalysts may also reflect uncontrolled reactions.

Cyclohexane yielded an almost equimolar mixture of cyclohexanol and cyclohexanone, which is consistent with the involvement of free radicals;[29] so is the decrease of the yields observed under anaerobic conditions (data not reported). Again, homolytic FeO−OH cleavage to yield hydroxyl radicals can be evoked to account for cyclohexane oxidation. In addition, the relative efficiency of **4b** vs **4a** can be correlated with the amount $Fe^{III}(OOH)$ that can be formed.

A nearly stoichiometric amount of PhIO vs Fe^{II} allowed to generate $Fe^{IV}(O)$ intermediates (see above). Therefore, the results given in Table 2 are close to single turnover oxidation of hydrocarbons by $Fe^{IV}(O)$ species.

Such species are able to oxidize the strong C−H bond of cyclohexane, as already reported for a handful of $Fe^{IV}(O)$ intermediates.[18a,23,30] However, only very small amounts of cyclohexanol were detected for **4a** and **4b**. Regarding anisole oxidation, no product arising from aromatic hydroxylation was obtained, but a small amount of phenol resulting from oxidative demethylation was observed. These results were quite expected.

dx.doi.org/10.1021/ic301834x | *Inorg. Chem.* 2013, 52, 691−700

Scheme 3[a]

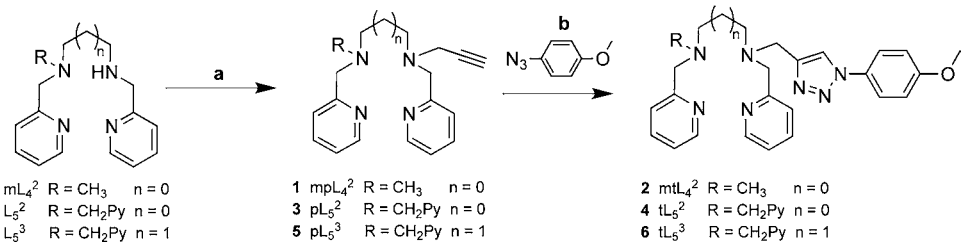

[a]Reagents and conditions: (a) propargyl bromide, K_2CO_3, THF, r.t., 16h (b) $CuSO_4$, sodium ascorbate, CH_2Cl_2/H_2O (1:1, v/v), r.t.

Indeed, the parent complexes of those catalysts generally displayed similar behavior.[2] In contrast, cyclooctene oxide was obtained with very good yields with the three complexes. As shown recently by Ye et al.,[31] $Fe^{IV}(O)$ intermediates are competent for alkene epoxidation. Thus, we propose that the oxoferryl generated from **4a** and **4b** are good epoxidizing agents. Precedents have been reported in the literature since yields between 15 and 35% were observed with the ligands L_5^3, TPEN, TPA and $L_6^2$4E.[2,18a,32] As far as we know, the results obtained here are the best reported for $Fe^{IV}(O)$ intermediates supported by a pentadentate amine/pyridine coordination sphere. This observation may be related to the relative stability of the oxidizing complexes. Indeed, the half-lives of $[(TPEN)Fe^{IV}(O)]^{2+}$ and $[(L_6^2 4E)Fe^{IV}(O)]^{2+}$ were estimated to be 30 and 42 min in acetonitrile at room temperature, respectively, whereas it is about 45 min for $[(tL_5^2)Fe^{IV}(O)]^{2+}$ generated from **4b** but at lower temperature (i.e., 0 °C, cf. Figure 5). Therefore, the oxidizing power of these complexes seems to be inversely correlated with their stability.[33] However, concluding in that sense or another, and determining the role played by the triazolyl moiety, if any, will require a more systematic study.

CONCLUSION

In this report, we have undertaken the coordination chemistry of Fe^{II} complexes with original mixed amine/pyridine/triazole ligands. In particular, we aimed at determining whether the flexible triazole fragment could be a competing ligand with respect to pyridyl and anions. In acetonitrile solution, the Fe^{III}/Fe^{II} redox potential appears to be a convenient probe to determine accurately the nature of the sixth ligand in complexes where a pentadentate amine/pyridine ligand is bound to the metal otherwise. Thus, the methoxyphenyltriazole moiety exhibits similar but somehow weaker donating ability than the pyridyl group. In addition, its coordination to Fe^{II} is effective but disfavored in the presence of metallophilic anions such as chlorides. Finally, in acetonitrile the stability of the complexes follows the order $[L_5Fe^{II}\text{-py}]^{2+} > [L_5Fe^{II}\text{–Cl}]^{+} > [L_5Fe^{II}\text{-triazolyl}]^{2+} > [L_5Fe^{II}\text{-(NCMe)}]^{2+}$, where L_5 designates a pentadentate coordination sphere composed of the two amines of ethanediamine and three pyridines. In contrast, for complexes based on propanediamine, the order is $[L_5Fe^{II}\text{–Cl}]^{+} > [L_5Fe^{II}(OTf)]^{+} > [L_5Fe^{II}\text{-(NCMe)}]^{2+}$, and no ligand exchange is observed for $[L_5Fe^{II}\text{-triazolyl}]^{2+}$.

Intermediates formed by reaction between chemical oxidants and two close complexes have been performed in which the methoxyphenyltriazole is coordinated to Fe^{II} or pendent and substituted by a chloride. For both complexes the same $Fe^{III}(OOH)$ is obtained with hydrogen peroxide, and the same $Fe^{IV}(O)$ is obtained with iodosylbenzene. These results are quite similar to those reported for their parent complexes and, therefore, indicate that the triazole does not modify the reactivity of the Fe^{II} precursors. In line with the ability of the different donors, it is quite clear that triazole does not bind to the metal center in the reaction intermediates. Accordingly, small molecule oxidation by hydrogen peroxide or iodosylbenzene in the presence of these complexes is in agreement with the one of $Fe^{III}(OOH)$ and $Fe^{IV}(O)$ inferred from previous studies. In particular, a great efficiency for the epoxidation of cyclooctene by PhIO is observed.

In conclusion, if ligand functionalization via "click chemistry" is envisioned, the so-obtained triazole moiety in place of a non coordinating group such as an alkyl, does not appear to modify the reactivity and the catalytic activity of Fe^{II} complexes. Therefore, lots of applications, such as surface grafting or introduction of a second sphere coordination function, may emerge for this family of catalysts.

EXPERIMENTAL SECTION

Commercially available chemicals were used without further purification unless stated otherwise. Solvents for electrochemical, spectroscopic measurements and catalysis experiments were purified by distillation, under argon, over CaH_2 for acetonitrile and over Mg for methanol. Ligands and complexes syntheses were carried out under argon atmosphere.

Ligands Syntheses. As previously described,[15,21,34] starting amine ligands were synthesized by reaction of *N,N′*-bis(2-pyridyl-methyl)-1,2-diaminoethane with formaldehyde to give mL_4^2. Use of 2-carboxaldehydepyridine instead of formaldehyde with *N,N′*-bis(2-pyridyl-methyl)-1,2-diaminoethane or *N,N′*-bis(2-pyridyl-methyl)-1,3-diaminopropane led to L_5^2 or L_5^3, respectively. Nucleophilic substitution of secondary amine ligands with propargyl bromide according to Huang et al. procedure gave access to corresponding mpL_4^2, mpL_4^3, pL_5^2, pL_5^3 ligands (Scheme 3).[35] 1-Azido-4-methoxybenzene was synthesized according to a reported procedure.[36]

Complex Syntheses. General procedure for $LFeCl_2$: under argon, a solution of $FeCl_2{\cdot}2H_2O$ (0.2 mmol) in ethanol (5 mL) was added to a stirred solution of L (0.2 mmol) in ethanol (5 mL). Cooling down the mixture overnight yielded a precipitate. After filtration, the solid was washed with diethyl ether (5 mL) and dried under vacuum.

General procedure for $[LFeCl](PF_6)$: a solution of $FeCl_2{\cdot}2H_2O$ (0.2 mmol) in ethanol (3 mL) was added to a solution of L (0.2 mmol) in ethanol (3 mL) under argon. To the brown solution the addition of a $NaPF_6$ (0.21 mmol) ethanolic solution (3 mL) and cooling down the mixture overnight resulted in a yellowish-brown precipitate. After filtration, the solid was washed with diethyl ether (5 mL) and dried under vacuum.

General procedure for $[LFe](PF_6)_2$: in a glovebox, a solution of $Fe(OTf)_2{\cdot}2MeCN$ (0.2 mmol) in ethanol (5 mL) was added to a stirred solution of L (0.2 mmol) in ethanol (5 mL). After stirring for 30 min, a solution of $NaPF_6$ (0.42 mmol) in ethanol (5 mL) was added to the mixture. After stirring overnight, the solution was filtered off. The solid was washed with diethyl ether (5 mL) and dried under vacuum.

dx.doi.org/10.1021/ic301834x | *Inorg. Chem.* 2013, 52, 691−700

[(pL_5^2)Fe(OTf)](OTf) **3b**. In a glovebox, a solution of Fe(OTf)$_2$·2MeCN (0.27 mmol, 0.12 g) in acetonitrile/ethanol (1/1 mL) was added to a stirred solution of pL_5^2 (0.27 mmol, 0.1 g) in ethanol (5 mL). The addition of diethyl ether and acetonitrile resulted in a color change of the solution from brown to yellow. Cooling down the mixture at 4 °C gave a precipitate. The solid was filtered off, washed with diethyl ether (5 mL), and dried under vacuum to afford a brown powder in 49% yield (0.10 g).

[(pL_5^3)Fe(OTf)](OTf) **5b**. In a glovebox, a solution of Fe(OTf)$_2$·2MeCN (0.26 mmol, 0.11 g) in ethanol (5 mL) was added to a stirred solution of pL_5^3 (0.26 mmol, 0.1 g) in ethanol (5 mL). The mixture was cooled down to −12 °C to yield yellow crystals suitable for X-ray crystallography (0.081 g, 42% yield).

Catalytic Assays. Conditions were Fe^{II}/H_2O_2 or PhIO/substrate: 1/20 or 2/800 (cyclohexane and cyclooctene) or 3000 (anisole) in freshly distilled acetonitrile solvent,. The total concentration in Fe was 1 mM. PhIO was added prior the substrate to ensure the formation of the Fe^{IV}(O) complex. Note that the oxidant was previously dissolved in the minimum amount of methanol, which did not impact the concentration in the reactants.

X-ray Crystallography. X-ray diffraction data for **1a** (mpL_4^2)FeCl$_2$, **3a** [(pL_5^2)FeCl](PF$_6$), **5a** [(pL_5^3)FeCl](PF$_6$), **4b** [(tL_5^2)Fe](PF$_6$)$_2$, **6b** [(tL_5^3)Fe](PF$_6$)$_2$, and **5b** [(pL_5^3)Fe(OTf)](OTf) were collected by using a Kappa X8 APPEX II Bruker diffractometer with graphite-monochromated $Mo_{K\alpha}$ radiation (λ = 0.71073 Å). Crystals were mounted on a CryoLoop (Hampton Research) with Paratone-N (Hampton Research) as cryoprotectant and then flashfrozen in a nitrogen-gas stream at 100 K. The temperature of the crystal was maintained at the selected value (100 K) by means of a 700 series Cryostream cooling device to within an accuracy of ±1 K. The data were corrected for Lorentz polarization, and absorption effects. The structures were solved by direct methods using SHELXS-97[37] and refined against F^2 by full-matrix least-squares techniques using SHELXL-97[38] with anisotropic displacement parameters for all non-hydrogen atoms. Hydrogen atoms were located on a difference Fourier map and introduced into the calculations as a riding model with isotropic thermal parameters. All calculations were performed by using the Crystal Structure crystallographic software package WINGX.[39]

The absolute configuration was determined by refining the Flack[40] parameter using a large number of Friedel's pairs.

The crystal data collection and refinement parameters are given in Supporting Information.

CCDC 890269−890274 contains the supplementary crystallographic data for this paper. These data can be obtained free of charge from the Cambridge Crystallographic Data Centre via www.ccdc.cam.ac.uk/data_ request/cif.

UV−visible. Electronic absorption spectra were recorded with a Varian Cary 50 spectrophotometer equipped with a Hellma immersion probe (1 cm optical path length) and fiber-optic cable. For low temperature experiments, a Thermo Haake CT90L cryostat was used.

Gas chromatography was performed on a Varian 430-GC equipped with a PDMS VF-1 ms column (15 m × 0.25 mm).

ESI-MS experiments were carried out with a Bruker Daltonics MicrOTOFq mass spectrometer in positive mode acquisition. Sample solutions prepared in acetonitrile or MeOH at a concentration of about 1 mM were infused at a flow rate of 10 μL min^{-1} with a CIL Cluzeau (Courbevoie, France) syringe. Solutions of Fe^{IV}(O) intermediates were frozen in liquid nitrogen and thawed just before injection.

EPR spectra were recorded at 9 GHz with a Bruker ELEXSYS 500 spectrometer equipped with a continuous flow Oxford E900 cryostat.

Electrochemical measurements were performed with an Autolab electrochemical workstation. The solvents were distilled under argon in the presence of CaH_2 and the solution (2 mmol L^{-1} for complexes and 0.1 mol·L^{-1} of $TBAPF_6$) introduced within an argon-purged heart-shaped cell. Cyclic voltammetry was performed using a glassy carbon electrode (3 mm in diameter) as the working electrode and a saturated calomel electrode as the reference (E_{ref} = 0.24 V/NHE). The low temperature was conducted using a Julabo FP 50 cryostat.

■ ASSOCIATED CONTENT

Ⓢ Supporting Information

Detailed synthetic procedures. Details of X-ray structural analysis for complexes **1a** (mpL_4^2)FeCl$_2$, **3a** [(pL_5^2)FeCl](PF$_6$), **4b** [(tL_5^2)Fe](PF$_6$)$_2$, **5a** [(pL_5^3)FeCl](PF$_6$), **5b** [(pL_5^3)Fe(OTf)](OTf), and **6b** [(tL_5^3)Fe](PF$_6$)$_2$, additional UV−visible, electrochemical, EPR, electrochemical and ESI-MS data. This material is available free of charge via the Internet at http://pubs.acs.org.

■ AUTHOR INFORMATION

Corresponding Author

*E-mail: jean-noel.rebilly@parisdescartes.fr (J.-N.R.), frederic.banse@u-psud.fr (F.B.).

Notes

The authors declare no competing financial interest.

■ REFERENCES

(1) (a) Girerd, J. J.; Banse, F.; Simaan, A. J. *Struct. Bonding (Berlin)* **2000**, *97*, 145. (b) Korendovych, I. V.; Kryatov, S. V.; Rybak-Akimova, E. V. *Acc. Chem. Res.* **2007**, *40*, 510. (c) Prat, I.; Mathieson, J. S.; Guell, M.; Ribas, X.; Luis, J. M.; Cronin, L.; Costas, M. *Nat. Chem.* **2011**, *3*, 788. (d) Que, L., Jr. *Acc. Chem. Res.* **2007**, *40*, 493. (e) Seo, M. S.; Kim, N. H.; Cho, K. B.; So, J. E.; Park, S. K.; Clemancey, M.; Garcia-Serres, R.; Latour, J. M.; Shaik, S.; Nam, W. *Chem. Sci.* **2011**, *2*, 1039.

(2) (a) Martinho, M.; Banse, F.; Bartoli, J.-F.; Mattioli, T. A.; Battioni, P.; Horner, O.; Bourcier, S.; Girerd, J.-J. *Inorg. Chem.* **2005**, *44*, 9592. (b) Thibon, A.; Bartoli, J.-F.; Bourcier, S.; Banse, F. *Dalton Trans.* **2009**, 9587.

(3) Collins, T. J. *Acc. Chem. Res.* **2002**, *35*, 782.

(4) Jollet, V. Ph.D. Thesis, n° d'ordre 10491, University Paris Sud, Orsay, France, 2011.

(5) Rostovtsev, V. V.; Green, L. G.; Fokin, V. V.; Sharpless, K. B. *Angew. Chem., Int. Ed.* **2002**, *41*, 2596.

(6) (a) Collman, J. P.; Devaraj, N. K.; Decreau, R. A.; Yang, Y.; Yan, Y. L.; Ebina, W.; Eberspacher, T. A.; Chidsey, C. E. D. *Science* **2007**, *315*, 1565. (b) Decréau, R. A.; Collman, J. P.; Yang, Y.; Yan, Y.; Devaraj, N. K. *J. Org. Chem.* **2007**, *72*, 2794. (c) Devaraj, N. K.; Dinolfo, P. H.; Chidsey, C. E. D.; Collman, J. P. *J. Am. Chem. Soc.* **2006**, *128*, 1794. (d) Gomila, A.; Le Poul, N.; Cosquer, N.; Kerbaol, J. M.; Noel, J. M.; Reddy, M. T.; Jabin, I.; Reinaud, O.; Conan, F.; Le Mest, Y. *Dalton Trans.* **2010**, *39*, 11516. (e) Schweinfurth, D.; Demeshko, S.; Khusniyarov, M. M.; Dechert, S.; Gurram, V.; Buchmeiser, M. R.; Meyer, F.; Sarkar, B. *Inorg. Chem.* **2012**, *51*, 7592.

(7) (a) Hao, E. R.; Wang, Z. Y.; Jiao, L. J.; Wang, S. W. *Dalton Trans.* **2010**, *39*, 2660. (b) Ostermeier, M.; Berlin, M. A.; Meudtner, R. M.; Demeshko, S.; Meyer, F.; Limberg, C.; Hecht, S. *Chem.—Eur. J.* **2010**, *16*, 10202. (c) Li, Y. J.; Huffman, J. C.; Flood, A. H. *Chem. Commun.* **2007**, 2692.

(8) Abbreviations used. TAML: tetraamido macrocyclic ligands; TPEN: *N*,*N*,*N*′,*N*′-tetrakis(2-pyridylmethyl)ethane-1,2-diamine); $L_6^2$4E: *N*,*N*,*N*′,*N*′-tetrakis(5-ethyl-2-pyridylmethyl)ethane-1,2-diamine; $m_2L_4^2$: *N*,*N*′-dimethyl-*N*,*N*′-bis(2-pyridylmethyl)-1,2-diaminoethane; mL_5^2: *N*-methyl-*N*,*N*′,*N*′-tris(2-pyridylmethyl)-1,2-diaminoethane; mpL_4^2: *N*-Methyl-*N*′-(prop-2-ynyl)-*N*,*N*′-bis-(pyridin-2-ylmethyl)-ethane-1,2-diamine; mtL_4^2: *N*-Methyl-*N*′-(1-(4-Methoxyphenyl)-1*H*-[1,2,3]triazol-4-ylmethyl)-*N*,*N*′-bis-(pyridin-2-ylmethyl)-ethane-1,2-diamine; pL_5^2: *N*-(Prop-2-ynyl)-*N*,*N*′,*N*′-tris-(pyridin-2-ylmethyl)-ethane-1,2-diamine; tL_5^2: *N*-(1-(4-Methoxy-phenyl)-1*H*-[1,2,3]triazol-4-ylmethyl)-*N*,*N*′,*N*′-tris-(pyridin-2-ylmethyl)-ethane-1,2-diamine; pL_5^3: *N*-(Prop-2-ynyl)-*N*,*N*′,*N*′-tris-(pyridin-2-ylmethyl)-propane-1,3-diamine; tL_5^3: *N*-(1-(4-Methoxy-phenyl)-1*H*-[1,2,3]triazol-4-ylmethyl)-*N*,*N*′,*N*′-tris-(pyridin-2-ylmethyl)-propane-1,3-diamine; TPA: tris(2-pyridylmethyl)amine; N4Py: *N*,*N*-bis(2-pyridylmethyl)-bis(2-pyridyl)methylamine.

(9) (a) Balland, V.; Banse, F.; Anxolabehere Mallart, E.; Nierlich, M.; Girerd, J. J. *Eur. J. Inorg. Chem.* **2003**, 2529. (b) Mialane, P.;

Novorojkine, A.; Pratviel, G.; Azéma, L.; Slany, M.; Godde, F.; Simaan, A.; Banse, F.; Kargar-Grisel, T.; Bouchoux, G.; Sainton, J.; Horner, O.; Guilhem, J.; Tchertanova, L.; Meunier, B.; Girerd, J. J. *Inorg. Chem.* **1999**, *38*, 1085.
(10) Chang, H. R.; Mccusker, J. K.; Toftlund, H.; Wilson, S. R.; Trautwein, A. X.; Winkler, H.; Hendrickson, D. N. *J. Am. Chem. Soc.* **1990**, *112*, 6814.
(11) Raffard, N.; Balland, V.; Simaan, J.; Letard, S.; Nierlich, M.; Miki, K.; Banse, F.; Anxolabehere-Mallart, E.; Girerd, J. J. *C. R. Chim.* **2002**, *5*, 99.
(12) Simaan, A. J.; Poussereau, S.; Blondin, G.; Girerd, J. J.; Defaye, D.; Philouze, C.; Guilhem, J.; Tchertanov, L. *Inorg. Chim. Acta* **2000**, *299*, 221.
(13) Roelfes, G.; Vrajmasu, V.; Chen, K.; Ho, R. Y. N.; Rohde, J. U.; Zondervan, C.; la Crois, R. M.; Schudde, E. P.; Lutz, M.; Spek, A. L.; Hage, R.; Feringa, B. L.; Munck, E.; Que, L., Jr. *Inorg. Chem.* **2003**, *42*, 2639.
(14) Bernal, I.; Jensen, I. M.; Jensen, K. B.; McKenzie, C. J.; Toftlund, H.; Tuchagues, J. P. *J. Chem. Soc., Dalton Trans.* **1995**, 3667.
(15) Balland, V.; Banse, F.; Anxolabehere-Mallart, E.; Ghiladi, M.; Mattioli, T. A.; Philouze, C.; Blondin, G.; Girerd, J. J. *Inorg. Chem.* **2003**, *42*, 2470.
(16) (a) Suijkerbuijk, B. M. J. M.; Aerts, B. N. H.; Dijkstra, H. P.; Lutz, M.; Spek, A. L.; van Koten, G.; Gebbink, R. J. M. K. *Dalton Trans.* **2007**, 1273. (b) Colasson, B.; Le Poul, N.; Le Mest, Y.; Reinaud, O. *Inorg. Chem.* **2011**, *50*, 10985.
(17) (a) Simaan, A. J.; Banse, F.; Girerd, J. J.; Wieghardt, K.; Bill, E. *Inorg. Chem.* **2001**, *40*, 6538. (b) Simaan, A. J.; Döpner, S.; Banse, F.; Bourcier, S.; Bouchoux, G.; Boussac, A.; Hildebrandt, P.; Girerd, J.-J. *Eur. J. Inorg. Chem.* **2000**, 1627.
(18) (a) Balland, V.; Charlot, M. F.; Banse, F.; Girerd, J. J.; Mattioli, T. A.; Bill, E.; Bartoli, J. F.; Battioni, P.; Mansuy, D. *Eur. J. Inorg. Chem.* **2004**, 301. (b) Klinker, E. J.; Kaizer, J.; Brennessel, W. W.; Woodrum, N. L.; Cramer, C. J.; Que, L., Jr. *Angew. Chem., Int. Ed.* **2005**, *44*, 3690.
(19) Balland, V.; Mathieu, D.; Pons, Y. M. N.; Bartoli, J. F.; Banse, F.; Battioni, P.; Girerd, J. J.; Mansuy, D. *J. Mol. Catal. A* **2004**, *215*, 81.
(20) Martinho, M.; Dorlet, P.; Riviere, E.; Thibon, A.; Ribal, C.; Banse, F.; Girerd, J.-J. *Chem.—Eur. J.* **2008**, *14*, 3182.
(21) Martinho, M.; Banse, F.; Sainton, J.; Philouze, C.; Guillot, R.; Blain, G.; Dorlet, P.; Lecomte, S.; Girerd, J. J. *Inorg. Chem.* **2007**, *46*, 1709.
(22) (a) Jaafar, H.; Vileno, B.; Thibon, A.; Mandon, D. *Dalton Trans.* **2011**, *40*, 92. (b) Mekmouche, Y.; Menage, S.; Pecaut, J.; Lebrun, C.; Reilly, L.; Schuenemann, V.; Trautwein, A.; Fontecave, M. *Eur. J. Inorg. Chem.* **2004**, *15*, 3163.
(23) Kaizer, J.; Klinker, E. J.; Oh, N. Y.; Rohde, J. U.; Song, W. J.; Stubna, A.; Kim, J.; Munck, E.; Nam, W.; Que, L., Jr. *J. Am. Chem. Soc.* **2004**, *126*, 472.
(24) Costas, M.; Mehn, M. P.; Jensen, M. P.; Que, L., Jr. *Chem. Rev.* **2004**, *104*, 939.
(25) Thibon, A.; Bartoli, J.-F.; Guillot, R.; Sainton, J.; Martinho, M.; Mansuy, D.; Banse, F. *J. Mol. Catal. A* **2008**, *287*, 115.
(26) Thibon, A.; Jollet, V.; Ribal, C.; Sénéchal-David, K.; Billon, L.; Sorokin, A. B.; Banse, F. *Chem.—Eur. J.* **2012**, *18*, 2715.
(27) (a) Chen, K.; Costas, M.; Kim, J. H.; Tipton, A. K.; Que, L., Jr. *J. Am. Chem. Soc.* **2002**, *124*, 3026. (b) Chen, K., Jr.; L., Q. *Angew. Chem., Int. Ed.* **1999**, *38*, 2227. (c) Talsi, E. P.; Bryliakov, K. P. *Coord. Chem. Rev.* **2012**, *256*, 1418.
(28) Bukowski, M. R.; Comba, P.; Lienke, A.; Limberg, C.; de Laorden, C. L.; Mas-Balleste, R.; Merz, M.; Que, L., Jr. *Angew. Chem., Int. Ed.* **2006**, *45*, 3446.
(29) Russell, G. A. *J. Am. Chem. Soc.* **1957**, *79*, 3871.
(30) Van den Berg, T. A.; de Boer, J. W.; Browne, W. R.; Roelfes, G.; Feringa, B. L. *Chem. Commun.* **2004**, *22*, 2550.
(31) Ye, W. H.; Ho, D. M.; Friedle, S.; Palluccio, T. D.; Rybak-Akimova, E. V. *Inorg. Chem.* **2012**, *51*, 5006.
(32) Lim, M. H.; Rohde, J. U.; Stubna, A.; Bukowski, M. R.; Costas, M.; Ho, R. Y. N.; Munck, E.; Nam, W.; Que, L., Jr. *Proc. Natl. Acad. Sci. U.S.A.* **2003**, *100*, 3665.
(33) Note that $Fe^{IV}(O)$ intermediates generated from precursors **4a** and **6b** cannot be directly compared as they could only be observed at a much lower temperature, i.e., −35 °C.
(34) Hureau, C.; Groni, S.; Guillot, R.; Blondin, G.; Duboc, C.; Anxolabehere-Mallart, E. *Inorg. Chem.* **2008**, *47*, 9238.
(35) Huang, S.; Clark, R. J.; Zhu, L. *Org. Lett.* **2007**, *9*, 4999.
(36) Zhu, W.; Ma, D. W. *Chem. Commun.* **2004**, 888.
(37) Sheldrick, G. M. *SHELXS-97, Program for Crystal Structure Solution*; University of Göttingen: Göttingen, Germany, 1997.
(38) Sheldrick, G. M. *SHELXL-97, Program for the Refinement of Crystal Structures*; University of Göttingen: Göttingen, Germany, 1997.
(39) Farrugia, L. J. *J. Appl. Crystallogr.* **1999**, *32*, 837.
(40) Flack, H. D. *Acta Crystallogr.* **1983**, *A39*, 876.